ACS OMEGA

http://pubs.acs.org/journal/acsodf

Article

Antiproliferative Potential of Gloriosine: A Lead for Anticancer Drug Development

Bharat Goel, Biswajit Dey, Essha Chatterjee, Nancy Tripathi, Nivedita Bhardwaj, Sanjay Kumar, Santosh Kumar Guru, and Shreyans K. Jain*

Cite This: *ACS Omega* 2022, 7, 28994−29001

Read Online

ACCESS | Metrics & More | Article Recommendations | Supporting Information

ABSTRACT: Gloriosine, a colchicine-like natural product, is widely obtained from *Gloriosa superba* roots. Despite having remarkable anticancer potential, colchicine could not pave its way to the clinic, while gloriosine is yet to be investigated for its pharmacological effects. In the present work, 14 compounds, including gloriosine, were isolated from the *G. superba* roots and were characterized by NMR spectroscopy. Gloriosine (**11**) was evaluated for its antiproliferative activity against a panel of 15 human cancer cell lines of different tissues and normal breast cells. Gloroisine (**11**) displayed significant antiproliferative activity against various cancer cell lines selectively, with IC_{50} values ranging from 32.61 to 100.28 nM. Further, gloriosine (**11**) was investigated for its apoptosis-inducing ability and found to form apoptotic bodies. It also inhibited A549 cell migration in the wound healing assay. Finally, molecular docking studies were performed to explore the possible binding modes of gloriosine with the colchicine-binding site of tubulin protein. Our findings suggested that gloriosine might be a potential lead for anticancer drug discovery.

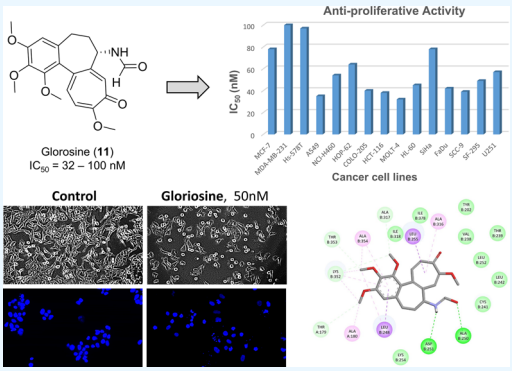

1. INTRODUCTION

Colchicine is a privileged natural product, obtained from *Colchicum autumnale* and *Gloriosa superba*, which has long been used for the treatment of gout, familial Mediterranean fever, and Behçet's disease. It exhibits potential antiproliferative activity by binding to the colchicine-binding site (CBS) at the interphase of α- and β-subunits of tubulin protein and inhibiting its self-assembly and microtubule polymerization, thereby arresting cell division.[1] Colchicine has also advanced into various stages of clinical trials for the treatment of different types of cancer and various cardiovascular disorders.[2] A semisynthetic derivative of colchicine, thiocolchicoside, is a muscle relaxant used clinically as an anti-inflammatory and analgesic drug.[3] Structurally, colchicine (**10**) consists of a trimethoxyphenyl ring (A), a cycloheptane ring (B), and a tropolone ring (C). Rings A and C are essential for binding to the CBS of tubulin.[4] The three methoxy groups at C-1, C-2, and C-3 of ring A play a crucial role in the high affinity of colchicine toward the CBS of tubulin protein. Although ring B is not essential for tubulin binding, it plays an important role in the kinetic properties of the colchicine−tubulin binding.[5] According to a computational study, the essential pharmacophoric features of CBS inhibitors are three hydrogen bond acceptors, one hydrogen bond donor, two hydrophobic centers, and one planar group.[6] Colchicine being the prototype of CBS inhibitors includes five of these features: two H-bond acceptors, two hydrophobic centers, and one planar group (Figure 1).

Tempering with the basic structure of colchicine results in loss of affinity toward the CBS. The relative positions of C-9 ketone and C-10 methoxy groups are important for the tubulin binding. Isocolchicine with reversed carbonyl and methoxy groups' relative position is inactive. Photoisomer of colchicine,

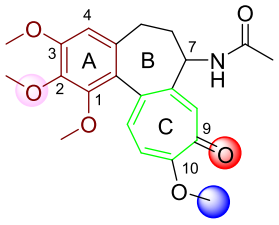

Figure 1. Pharmacophoric features of colchicine as colchicine-binding site (CBS) inhibitors. The red and pink points are hydrogen bond acceptors, the blue point and brown lines represent hydrophobic centers, and the green lines represent the planar group.

Received: April 30, 2022
Accepted: August 4, 2022
Published: August 12, 2022

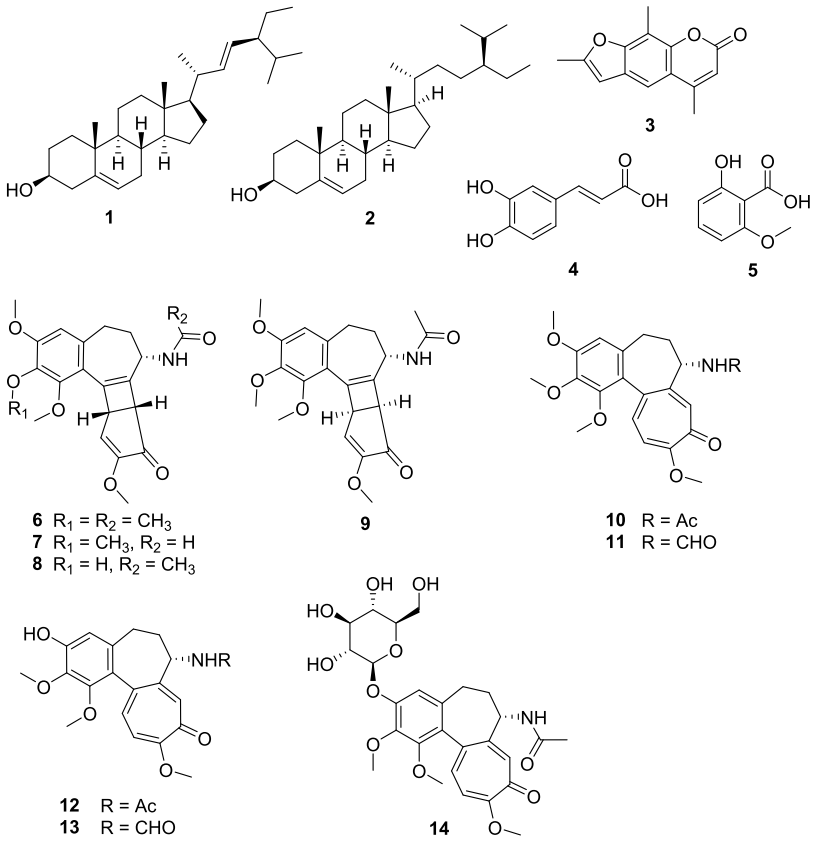

Figure 2. Chemical structures of compounds (**1**−**14**) isolated from the *G. superba* roots.

called lumicolchicine, possesses a transformed ring C (four- and five-membered ring fused system) and have reduced binding affinity toward tubulin.[7] Various semisynthetic modifications have been done to potentiate the anticancer activity of colchicine.[7,8]

Roots of *G. superba* are used for the commercial production of colchicine. Apart from colchicine, several other colchicine analogues have been reported to be isolated from *G. superba*, such as 3-demethylcolchicine, lumicolchicine, gloriosine, and colchicine glycosides.[9] The roots of *G. superba* are used traditionally in the Indian system of medicine for the treatment of gout, arthritis, rheumatic disorders, skin diseases, leprosy, ulcers, snakebite, impotency, *etc.*[10] Apart from the anticancer and cytotoxic activities, the *G. superba* extracts have shown many other bioactivities in laboratory experiments such as antimicrobial,[11] analgesic, anti-inflammatory,[12] antioxidant,[13] and inhibition of lipoxygenase, acetylcholinesterase, and butyrylcholinesterase enzymes.[14] In our quest to hunt for anticancer natural products, the roots and tubers of *G. superba* were investigated and 14 known compounds, including gloriosine, were isolated. Since gloriosine is structurally similar to colchicine and it has never been reported for its pharmacological effects, we carried out its preliminary cytotoxic screening in 15 human cancer cell lines of different tissues and one normal breast cell line. To better understand the interaction of gloriosine with tubulin protein, it was docked for the possible binding modes with the colchicine-binding site of tubulin protein. Gloriosine−tubulin binding was further validated by molecular dynamics simulation study.

2. RESULTS AND DISCUSSION

2.1. Phytochemistry of *G. superba* Roots. The dried roots of *G. superba* were extracted three times with chloroform/methanol (v/v, 1:1) at room temperature. The crude extract was concentrated under reduced pressure to evaporate the organic solvent. The dried extract was subjected to silica gel column chromatography. Repeated column chromatography led to the isolation of 14 compounds. All of the isolated compounds were characterized by matching with their reported ^{1}H and ^{13}C NMR values (Supporting Information). Isolated compounds were identified as stigmasterol (**1**),[15] *β*-sitosterol (**2**),[15] trioxsalen (**3**),[16] caffeic acid (**4**),[17] 6-methoxysalicylic acid (**5**),[18] *β*-lumicolchicine (**6**),[19] *N*-deacetyl-*N*-formyl-*β*-lumicolchicine (**7**),[20] 2-demethyl-*β*-lumicolchicine (**8**),[19] *γ*-lumicolchicine (**9**),[19] colchicine (**10**),[21] gloriosine (**11**),[22] 3-demethylcolchicine (**12**),[21] 3-demethyl-*N*-deacetyl-*N*-formyl colchicine (**13**),[22] and colchicoside (**14**)[23] (Figure 2).

Stigmasterol (**1**), *β*-sitosterol (**2**), trioxsalen (**3**), caffeic acid (**4**), and 6-methoxysalicylic acid (**5**) were nonalkaloidal common components widely obtained from various higher plant species. *β*-Lumicolchicine (**6**), *N*-deacetyl-*N*-formyl-*β*-lumicolchicine (**7**), 2-demethyl-*β*-lumicolchicine (**8**), and *γ*-lumicolchicine (**9**) were obtained as minor compounds. *β*- and *γ*-lumicolchicine are stereoisomers with the acetamide group at C-7 in *cis*- or *trans*-configuration to the five-membered ring (with ring A, ring B, and four-membered rings coplanar).[24] Both the isomers were distinguished on the basis of one-dimensional (1D) and two-dimensional (2D) NMR spectra.[19] Final structures of **6** and **9** were established by the NOESY experiments. In *β*-lumicolchicine (**6**), H-7 (δ_H 4.82 ppm) and

https://doi.org/10.1021/acsomega.2c02688
ACS Omega 2022, 7, 28994−29001

H-8 (δ_H 3.62 ppm) displayed spatial correlation in NOESY spectra, but this correlation was not observed in γ-lumicolchicine (**9**), confirming that in **6**, both H-7 and H-8 are *cis* to each other, whereas in **9**, these protons are *trans* (Sections S6 and S9, Supporting Information). Lumicolchicines are the isomers of colchicine in which ring C of colchicine is rearranged to a conjugated four- and five-membered ring system. Although lumicolchicines have been isolated from *G. superba* earlier, they may be artifacts because lumicolchicines have been reported to be produced as a result of photoisomerization of colchicine when exposed to UV light.

Similarly, *N*-deacetyl-*N*-formyl-β-lumicolchicine (**7**) perhaps derived from *N*-deacetyl-*N*-formyl colchicine under the photocatalytic condition. 3-Demethylcolchicine (**12**), 3-demethyl-*N*-deacetyl-*N*-formyl colchicine (**13**), and colchicoside (**14**) were obtained in minor amounts from the polar fractions of column. Repeated attempts were made to purify gloriosine (**11**) as it is closely associated with colchicine (**10**). The complete structure of gloriosine (**11**) was established by 2D NMR. To the best of our knowledge, this is the first report describing its structural features by NMR studies (Section S11, Supporting Information). Except for a few peaks, ^{1}H NMR and ^{13}C NMR spectra of **11** and **10** were very similar. In gloriosine (**11**), peaks due to the methyl group at δ_H 1.97 and δ_C 22.77 ppm disappeared, while an aldehyde proton was detected at δ_H 8.18 ppm. Also, the peak due to the aldehyde carbonyl group appeared at δ_C 160.89 ppm in place of δ_C 170.13 ppm (peak due to the acetamide carbonyl group). Based on these findings and validated by 2D NMR and MS spectra, it is confirmed that chemically gloriosine (**11**) is *N*-deacetyl-*N*-formyl-colchicine.

Despite its potential as an anticancer agent, colchicine has not been used clinically. Several factors limited the clinical use of colchicine as an anticancer drug such as colchicine that develops multidrug resistance due to its *p*-glycoprotein induction activity.[8a] Also, it has shown potential toxic effects like cardiotoxicity, neuropathy, and myopathy due to its toxicity.[25] Although gloriosine (**11**) is a well-known molecule, its chemistry and pharmacology have never been investigated. In the current study, it was collected in gram amount (the second major compound after colchicine). Hence, we decided to explore the anticancer pharmacology of gloriosine (**11**) with reference to colchicine, assuming it as a better lead.

2.2. *In Vitro* Antiproliferative Assay of Gloriosine (11). In the present work, gloriosine (**11**) was evaluated for its cytotoxic activity against a panel of 15 human cancer cell lines from various tissue origins as listed in Table 1, using the 3-(4,5-dimethylthiazol-2-yl)-2,5-diphenyltetrazolium bromide (MTT) assay. Colchicine (**10**) was used as the positive control. Surprisingly, **11** exhibited highly potent activity against all of the tested cancer cell lines with IC_{50} values ranging from 32.61 to 100.28 nM after 48 h while 700.48 nM in the case of normal breast cells (Table 1). The IC_{50} values of **11** were less than colchicine except in some cases. Gloriosine (IC_{50}: 700.48 nM) appears to be less toxic as compared to colchicine (IC_{50}: 567.81 nM) when tested in normal breast cells. Toxicity window in cancer cells and normal cells indicated that gloriosine (**11**) is less toxic to normal cells and more selective toward the cancer cells than colchicine (**10**).

2.3. Nuclear Staining and Fluorescence Microscopy. Gloriosine (**11**) has shown potent cytotoxicity against lung cancer cells, and further experiments were performed in A549 (lung) cells. To address the cause of cell death by gloriosine, nuclear morphological changes were studied by nuclear staining and fluorescence microscopy of A549 cells. A549 cells were treated with 50, 100, and 500 nM gloriosine (**11**) for 24 h. After the treatment, characteristic changes of apoptosis such as the formation of apoptotic bodies, nuclear condensation, and membrane blebbing were observed in the morphology of the treated cells in a concentration-dependent manner, whereas the untreated cells' nuclei were found to have a normal intact morphology. The results suggest that gloriosine (**11**) was able to induce an apoptotic cell morphology in A549 cells (Figure 3).

Table 1. IC_{50} Values (nM) of Gloriosine (11) and Colchicine (10) in Various Human Cancer Cell Lines and Normal Cell Line after 48 h

			IC_{50} ± SD (nM)	
s. no.	human cancer cell lines	tissue origin	gloriosine (**11**)	colchicine (**10**)[a]
1	MCF-7	breast	78.65 ± 6.23	110.74 ± 9.87
2	MDA-MB-231		100.28 ± 7.22	70.58 ± 9.67
3	Hs 578T		97.64 ± 6.99	90.16 ± 9.56
4	A549	lung	35.12 ± 2.43	40.30 ± 3.32
5	NCI-H460		54.55 ± 3.89	64.84 ± 5.21
6	HOP-62		64.43 ± 4.11	86.61 ± 6.96
7	COLO 205	colon	40.28 ± 2.36	120.06 ± 1.10
8	HCT 116		38.25 ± 2.09	140.00 ± 10.98
9	MOLT-4	leukemia	32.61 ± 2.88	ND[b]
10	HL-60		45.34 ± 3.67	ND
11	SiHa	cervix	78.87 ± 5.77	137.64 ± 12.78
12	FaDu	oral	42.37 ± 3.98	ND
13	SCC-9		39.25 ± 3.10	ND
14	SF-295	brain	49.50 ± 3.78	54.39 ± 3.499
15	U251		57.29 ± 4.11	76.83 ± 3.1
16	MCF-10A	normal breast	700.48 ± 27.89	567.81 ± 56.77

[a]Used as positive control. [b]Not determined.

2.4. Cell Migration Inhibition. To assess its effect on cell migration, a wound healing assay was performed to examine the chemotactic motility of A549 cells. At 500 nM concentration, gloriosine (**11**) completely inhibited the cell migration, which was more active than colchicine (Figure 4a). Gloriosine (**11**) was found to greatly impede cell migration in a concentration-dependent manner. It was observed that gloriosine (**11**) decreased the wound closure percentage from 85 to 11% at 500 nM concentration (Figure 4b).

2.5. Molecular Docking. Next, we performed the molecular docking studies of gloriosine (**11**) with tubulin protein (PDB: 4O2B) to study the possible binding modes of the colchicine-binding site. The binding energy for gloriosine (ligand) was found to be −8.06 kcal/mol for tubulin, which was almost equal to that of colchicine (−8.01 kcal/mol). Gloriosine showed important interactions with tubulin protein such as alkyl interaction with Ala180 of α-subunit, H-bond with Ala250 and Asp251 of β-subunit, and π-sigma bond with Leu255 and Leu248 of β-subunit (Figure 5A). The interactions of gloriosine with tubulin protein are represented in Figure 5 and Table S1. The root-mean-square deviation (RMSD) between the co-crystallized ligand and docked ligand was found to be 0.41 Å, indicating that the selected grid displayed less deviation and could be used for docking studies (Figure S48).

2.6. Molecular Dynamics Simulation of Gloriosine with Tubulin Protein. Molecular dynamics (MD) simulation

https://doi.org/10.1021/acsomega.2c02688
ACS Omega 2022, 7, 28994−29001

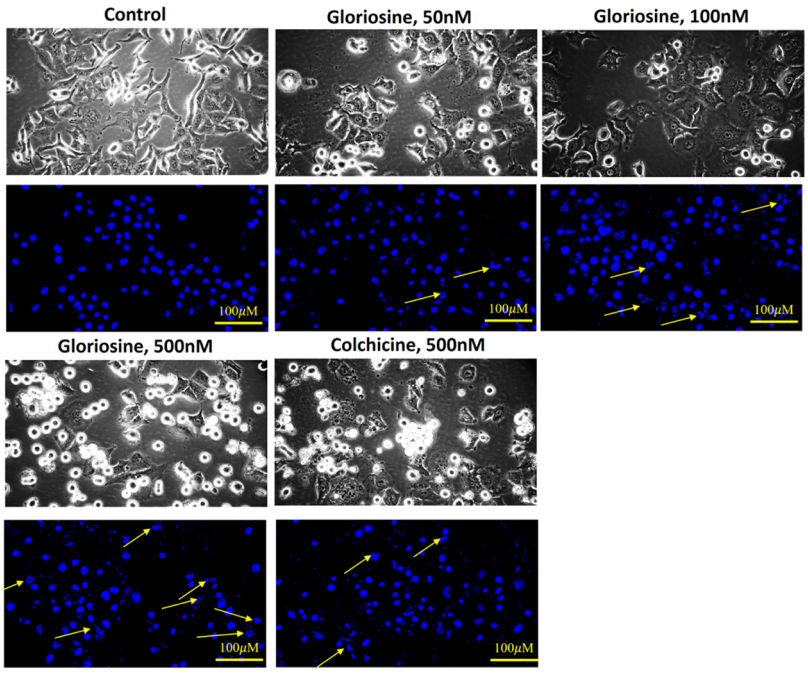

Figure 3. Nuclear staining after treatment with different concentrations (50, 100, and 500 nM) of gloriosine (**11**) and 500 nM of colchicine (**10**) on A549 cells for 24 h revealed the formation of apoptotic bodies in a dose-dependent manner.

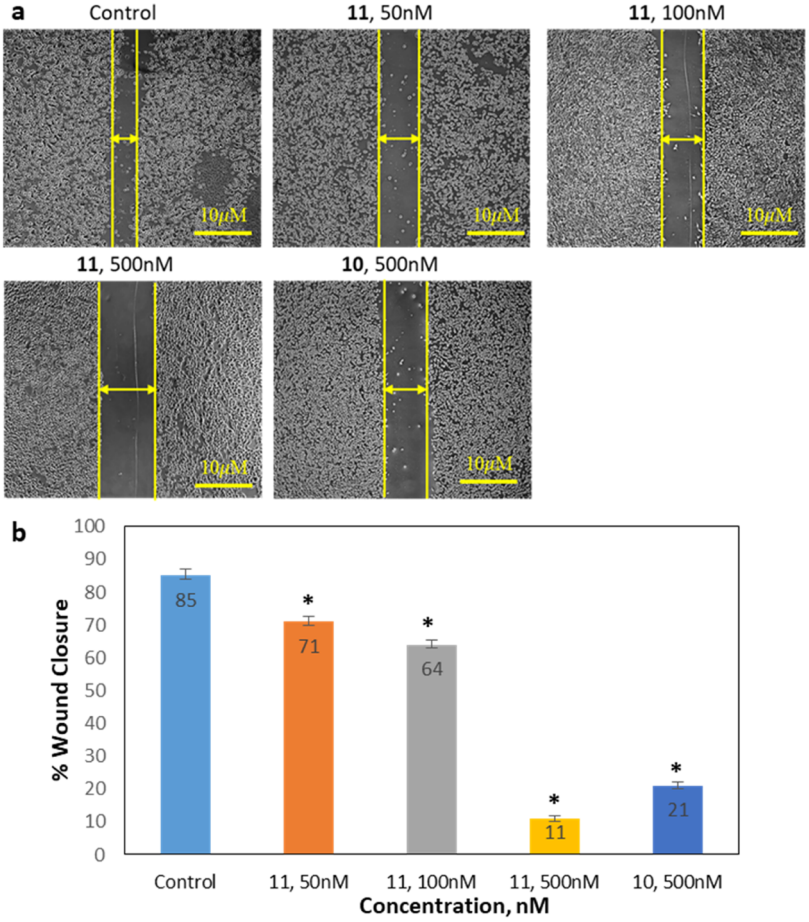

Figure 4. (a) Effect of gloriosine (**11**) and colchicine (**10**) on *in vitro* cell migration in A549 cells after 24 h. (b) Gloriosine (**11**) inhibited A549 cells migration in a dose-dependent manner.

is a computational method for studying the physical movement of atoms and molecules in a biophysical system. In this study, the MD simulation was done to establish the stability of the gloriosine−tubulin complex.

https://doi.org/10.1021/acsomega.2c02688
ACS Omega 2022, 7, 28994−29001

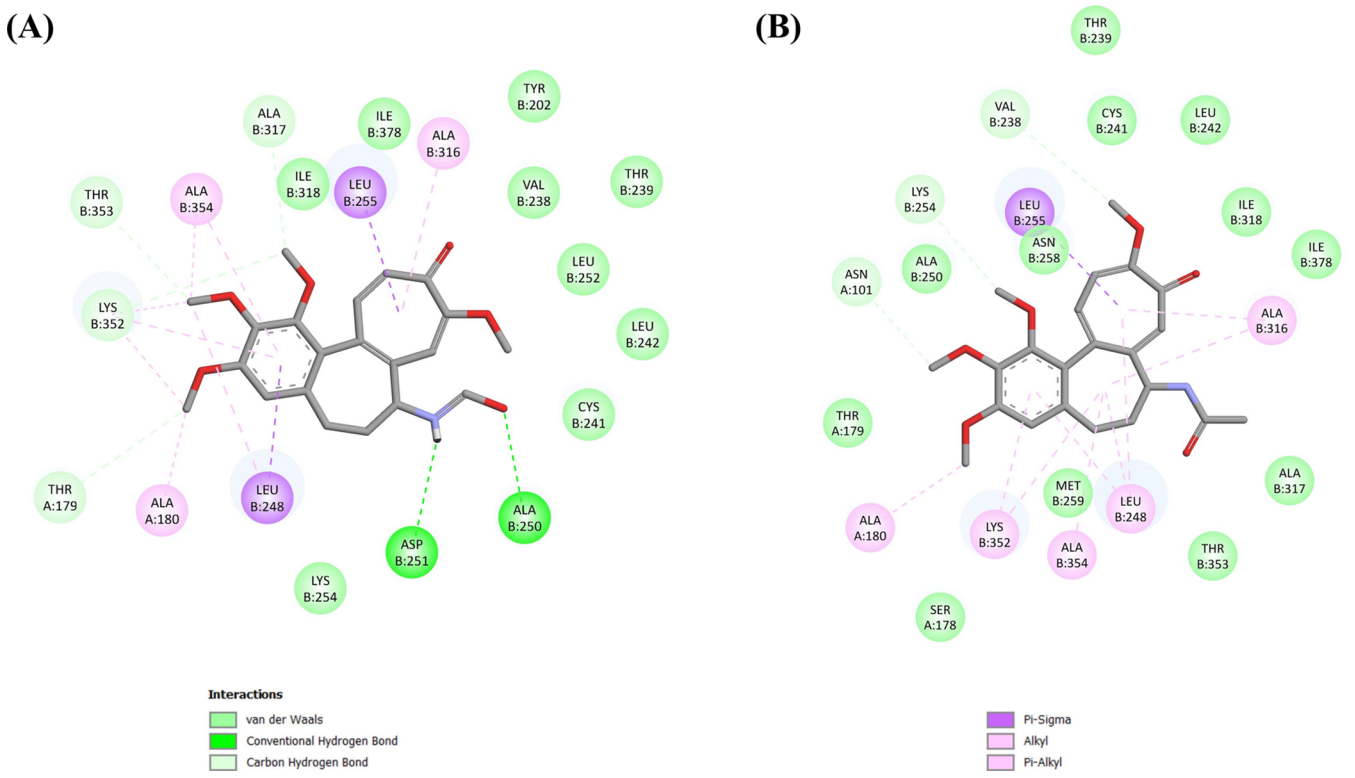

Figure 5. Protein−ligand interaction diagram of compounds (A) gloriosine and (B) colchicine against the colchicine-binding site of tubulin protein (PDB ID: 4O2B).

2.6.1. RMSD Analyses. The actual movement and structural changes of a protein in a biological environment can be visualized using MD simulations. The RMSD indicates the equilibration and stability of a complex.[26] It is evident from Figure 6 that the protein attains a stable RMSD during the simulation run. In the case of the gloriosine−tubulin complex, the maximum protein backbone RMSD was found to be 3.42 Å, which is considered perfectly fine for small and globular proteins. The average protein backbone RMSD was found to be 1.99 Å for the gloriosine−tubulin protein complex. In the same plot, it was observed that the ligand RMSD was not significantly larger than the protein RMSD, which indicates that the ligand does not diffuse away from the initial binding site. The average ligand RMSD was found to be 3.04 Å for the gloriosine−tubulin protein complex.

2.6.2. RMSF Analyses. The RMSF is useful for characterizing local changes along the protein chain. The peaks in the plot represent the residues, which fluctuates the most during the simulation. The RMSF analysis was calculated for the C-α atom of protein residues. The average protein RMSF was found to be 1.76 Å for the gloriosine−tubulin protein complex. The residues participating in interactions with ligands *i.e.*, Thr179, Leu255, Thr314, and Thr353, remained highly stable throughout the simulation.

2.6.3. H-Bond Interaction Analyses. Protein interactions with the ligand were monitored throughout the simulation. The H-bond interaction analysis is important to understand the stability of the predicted protein−ligand complex. H-bonding plays a significant role in accommodating the ligand inside the binding site. Gloriosine showed the H-bond interaction with Thr179, Leu255, and Thr314. Similar interactions were also observed in docking studies as well.

3. CONCLUSIONS

In conclusion, gloriosine displayed significant cytotoxic activity in all of the tested cancer cell lines with IC_{50} values of 32.61−100.28 nM. Gloriosine was found to be more active than colchicine in some of the cell lines. A mechanistic study revealed that gloriosine exhibited potential apoptotic and antimigratory activities in A549 cells. Finally, molecular docking and molecular dynamics simulation studies showed that gloriosine is bound to the colchicine-binding site of tubulin protein. Based on these preliminary results, gloriosine may serve as an interesting lead for future anticancer therapeutics.

4. EXPERIMENTAL SECTION

4.1. General Experimental Procedures. All chemicals were obtained from Sigma-Aldrich Company and used as received. ^{1}H and ^{13}C NMR spectra were recorded on Bruker-Avance III HD 500 and 125 MHz NMR instruments, respectively. Chemical shifts are reported in parts per million (ppm) downfield from tetramethylsilane (TMS) and are referenced to the residual proton/carbon in the NMR solvent ($CDCl_3$, 7.26:77.1 ppm; MeOD, 3.31:49.00 ppm; DMSO-d_6, 2.50:39.5 ppm). All chromatographic purifications were performed on silica gel (#60-120 or #100-200) obtained from Merck. Thin-layer chromatography (TLC) was performed on precoated silica gel 60 GF_{254} aluminum sheets (Merck) and visualized under UV light (254 nm) by spraying an anisaldehyde−sulfuric acid reagent followed by heating.

4.2. Plant Material. The dried roots and tubers of *G. superba* were purchased from the local market of Varanasi, India, in January 2020 and authenticated by Dr. Bikarma Singh. A specimen sample (accession number: RRLH57502)

https://doi.org/10.1021/acsomega.2c02688
ACS Omega 2022, 7, 28994−29001

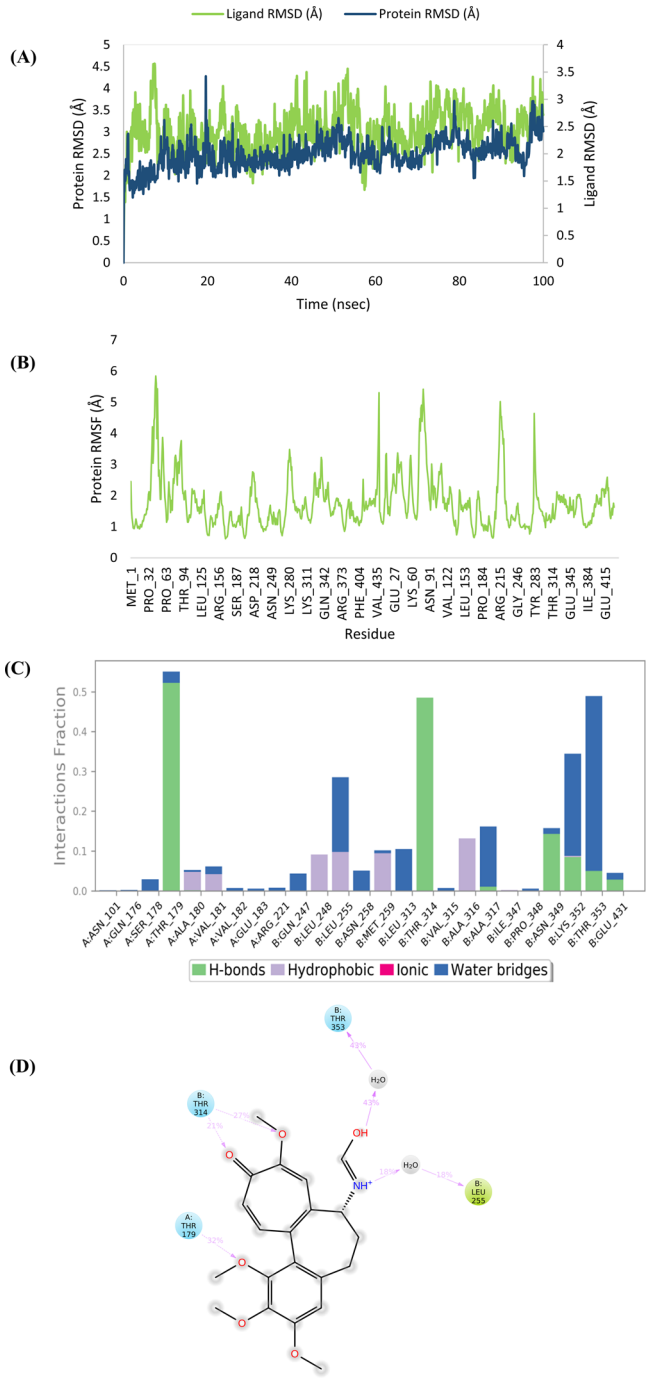

Figure 6. MD simulation of gloriosine complexed with tubulin. (A) RMSD plot of tubulin and gloriosine. (B) Root-mean-square fluctuation (RMSF) plot of tubulin. (C) Protein−ligand contacts between tubulin and gloriosine during a MD run. (D) Interactions of gloriosine with tubulin during a MD run.

was preserved in Janaki Ammal Herbarium at the CSIR-IIIM, Jammu, India.

4.3. Extraction and Isolation. The dried roots of *G. superba* (2 kg) were coarsely powdered and extracted three times (4 L, each) with chloroform/methanol (v/v, 1:1) at room temperature. The crude extract was filtered and evaporated to dryness *in vacuo* to yield 163 g of the semisolid material. The dried extract was chromatographed over silica gel (#100-200) and eluted with a *n*-hexane-ethyl acetate step gradient system (v/v, 1:0 → 0:1) and then with ethyl acetate/methanol (v/v, 1:0 → 9:1). First, the extract was defatted with hexane. With an increasing percentage of ethyl acetate (5%), stigmasterol and *β*-sitosterol were obtained. Further increasing the percentage of ethyl acetate in a step gradient manner afforded trioxsalen, caffeic acid, 6-methoxysalicylic acid, *β*-lumicolchicine, *N*-deacetyl-*N*-formyl-*β*-lumicolchicine, 2-demethyl-*β*-lumicolchicine, *γ*-lumicolchicine, colchicine, gloriosine, 3-demethylcolchicine, 3-demethyl-*N*-deacetyl-*N*-formyl colchicine, and colchicoside. All compounds were purified by repeated silica gel column chromatography.

4.4. Cell Culture and Growth Conditions. All cells lines were purchased from the National Cancer Institute (NCI), Bethesda, and cultured according to the provided protocol. The cells were grown in a CO_2 incubator (Esco) at 37 °C in a humidified atmosphere (98% humidity) of 95% air and 5% CO_2.

4.5. *In Vitro* Cytotoxicity Studies. The cytotoxicity study was performed using the 3-(4,5-dimethylthiazol-2-yl)-2,5-diphenyltetrazolium bromide (MTT) assay. In this assay, the cells were plated in a 96-well plate for 12 h. Then, the cells were treated with different concentrations (5, 10, 50, 100, and 500 nM) of gloriosine and colchicine for a duration of 48 h. After incubation, 10 μL of MTT dye (2.5 mg/mL in phosphate-buffered saline (PBS)) was added to each well and incubated for 4 h at 37 °C. Then, the supernatant was aspirated and purple MTT-formazan crystals obtained were dissolved in 150 μL of DMSO. The absorbance of this colored solution was measured at a wavelength of 570 nm.[15]

4.6. Nuclear Staining and Fluorescence Microscopy. A549 cells were treated with 50, 100, and 500 nM concentrations of gloriosine and 500 nM colchicine for 24 h. After the treatment, cells were collected, washed twice with PBS, and fixed in 400 μL of cold acetic acid/methanol (1:3, v/v) overnight at 4 °C. The next day, cells were washed and dispensed in 50 μL of fixing solution. After that, the cells were spread out on a clean slide and allowed to dry at room temperature overnight. The cells were stained with 4′,6-diamidino-2-phenylindole (DAPI) (5 μg/mL in 0.01 M citric acid and 0.45 M disodium phosphate containing 0.05% Tween 20) for 30 min at room temperature, and then, the slides were rinsed with distilled water followed by washing with PBS. While the slide was still wet, 40 μL of mounting fluid (PBS/glycerol, 1:1) was poured over it and then sealed with a glass coverslip. Cells were observed under a microscope for any nuclear morphological changes that occur during apoptosis. For phase-contrast microscopy, cells were simply photographed using a microscope after treatment.[15]

4.7. Scratch Assay for Migration Studies. The cell migration studies were performed in A549 cells. A549 cells were treated with mitomycin C to inactivate cell proliferation. The cells were scratched with a 200 μL sterile microtip and washed three times with phosphate-buffered saline (PBS), supplemented with fresh medium and treated with 50, 100, and 500 nM concentrations of gloriosine and 500 nM colchicine for 24 h. Images of the cells were taken after 24 h of incubation, and the percentage of wound closure was expressed with respect to the untreated cells.[27]

4.8. Molecular Docking. Molecular docking studies were performed using AutoDock 4.2 to study the molecular interactions between gloriosine and the colchicine-binding site of tubulin protein (PDB: 4O2B).[28] The crystal structure was retrieved from the protein data bank (https://www.rcsb.org/). The pdb2pqr web server was used to assign the right

https://doi.org/10.1021/acsomega.2c02688
ACS Omega 2022, 7, 28994−29001

protonation state to the residues. All of the water molecules, ligands, and ions were removed. Nonpolar hydrogen atoms were removed, and Gasteiger charges were added using M.G.L Tools 1.5.7.rc1. AutoDock employs Autogrid4 to compute maps. The docking study was performed using the Lamarckian genetic algorithm (LGA). The docking was performed with 100 runs, 150 population sizes, 27,000 number of generations, and 2,500,000 number of energy evaluations. It employs a "semiempirical free-energy force field" to evaluate conformations at the time of the docking simulation. The docking protocol validation was done by redocking the co-crystallized ligand and calculating RMSD between the docked pose and co-crystallized ligand. The docked pose was visualized by Discovery studio 2019 for studying interactions. Upon successful completion of the docking simulation, the best confirmation was selected with the best binding energy in the largest cluster of 2.0 Å.

4.9. Molecular Dynamics Simulation of the Gloriosine−Tubulin Complex. Molecular dynamics (MD) simulation of the gloriosine−tubulin complex was carried out using the Desmond package (D.E. Shaw Research, New York) with inbuilt optimized potentials for the liquid simulation (OPLS 2005) force field.[29] The gloriosine−tubulin complex was obtained from Autodock. Before performing the MD simulation, the solvated system was prepared. The complex was solvated using an open TIP3P water model in periodic boundary conditions of a cubic box with dimensions 12 × 12 × 12 $Å^3$. The overall negative charge of the system was neutralized by adding sodium ions. The desired electrically neutral system for simulation was built with 0.15 M NaCl. The relaxation of the system was performed by implementing the steepest descent and the limited memory Broyden−Fletcher−Goldfarb−Shanno algorithm with a threshold of 2.0 kcal/mol.[30] The simulation was performed under an NPT ensemble for 100 ns, implementing the Berendsen thermostat and barostat methods. A constant temperature of 310 K was maintained across the simulation run using the Noose−Hoover thermostat algorithm, and the pressure of 1 atm was maintained using the Martyna−Tobias−Klein barostat algorithm.[29,31] The cutoff value of 9.0 Å was set to analyze the short-range Coulombic interactions using the short-range method. The long-range Coulombic interactions were handled using the smooth particle mesh Ewald method. The tolerance value for long-range interactions was set to 10^{-9}, which was implemented by the SHAKE algorithm. The final production run was carried out for 100 ns, and the trajectory sampling was done at 100 ps. The trajectories obtained from the following MD run were analyzed for the protein and ligand RMSD, protein root-mean-square fluctuation (RMSF), and H-bond interactions.

■ ASSOCIATED CONTENT

Supporting Information

The Supporting Information is available free of charge at https://pubs.acs.org/doi/10.1021/acsomega.2c02688.

1D and 2D NMR spectroscopic data of compounds (**1**−**14**): S1. stigmasterol (**1**), S2. β-sitosterol (**2**), S3. trioxsalen (**3**), S4. caffeic acid (**4**), S5. 6-methoxysalicylic acid (**5**), S6. β-lumicolchicine (**6**), S7. *N*-deacetyl-*N*-formyl-β-lumicolchicine (**7**), S8. 2-demethyl-β-lumicolchicine (**8**), S9. γ-lumicolchicine (**9**), S10. colchicine (**10**), S11. gloriosine (**11**), S12. 3-demethylcolchicine (**12**), S13. 3-demethyl-*N*-deacetyl-*N*-formyl colchicine (**13**), S14. colchicoside (**14**) (PDF)

■ AUTHOR INFORMATION

Corresponding Author

Shreyans K. Jain − *Department of Pharmaceutical Engineering and Technology, Indian Institute of Technology (Banaras Hindu University), Varanasi 221005 Uttar Pradesh, India;* orcid.org/0000-0001-6160-8755; Email: sjain.phe@iitbhu.ac.in

Authors

Bharat Goel − *Department of Pharmaceutical Engineering and Technology, Indian Institute of Technology (Banaras Hindu University), Varanasi 221005 Uttar Pradesh, India;* orcid.org/0000-0002-6297-0067

Biswajit Dey − *Department of Biological Sciences, National Institute of Pharmaceutical Education and Research (NIPER), Hyderabad 500037 Telangana, India*

Essha Chatterjee − *Department of Biological Sciences, National Institute of Pharmaceutical Education and Research (NIPER), Hyderabad 500037 Telangana, India*

Nancy Tripathi − *Department of Pharmaceutical Engineering and Technology, Indian Institute of Technology (Banaras Hindu University), Varanasi 221005 Uttar Pradesh, India*

Nivedita Bhardwaj − *Department of Pharmaceutical Engineering and Technology, Indian Institute of Technology (Banaras Hindu University), Varanasi 221005 Uttar Pradesh, India*

Sanjay Kumar − *Department of Pharmaceutical Engineering and Technology, Indian Institute of Technology (Banaras Hindu University), Varanasi 221005 Uttar Pradesh, India*

Santosh Kumar Guru − *Department of Biological Sciences, National Institute of Pharmaceutical Education and Research (NIPER), Hyderabad 500037 Telangana, India*

Complete contact information is available at: https://pubs.acs.org/10.1021/acsomega.2c02688

Notes

The authors declare no competing financial interest.

■ ACKNOWLEDGMENTS

The authors are thankful to Dr. Bikarma Singh, Senior Scientist, CSIR-National Botanical Research Institute, Lucknow, Uttar Pradesh, for the authentication of the plant material. B.G., N.T., and N.B. acknowledge IIT (BHU), Varanasi, for providing Teaching Assistantship.

■ REFERENCES

(1) Kumar, A.; Sharma, P. R.; Mondhe, D. M. Potential anticancer role of colchicine-based derivatives: an overview. *Anti-Cancer Drugs* **2017**, *28*, 250−262.

(2) (a) Verma, S.; Eikelboom, J. W.; Nidorf, S. M.; Al-Omran, M.; Gupta, N.; Teoh, H.; Friedrich, J. O. Colchicine in cardiac disease: a systematic review and meta-analysis of randomized controlled trials. *BMC Cardiovasc. Disord.* **2015**, *15*, No. 96. (b) Deftereos, S.; Giannopoulos, G.; Papoutsidakis, N.; Panagopoulou, V.; Kossyvakis, C.; Raisakis, K.; Cleman, M. W.; Stefanadis, C. Colchicine and the Heart: Pushing the Envelope. *J. Am. Coll. Cardiol.* **2013**, *62*, 1817−1825.

(3) Carta, M.; Murru, L.; Botta, P.; Talani, G.; Sechi, G.; De Riu, P.; Sanna, E.; Biggio, G. The muscle relaxant thiocolchicoside is an antagonist of GABAA receptor function in the central nervous system. *Neuropharmacology* **2006**, *51*, 805−815.

(4) Hagras, M.; El Deeb, M. A.; Elzahabi, H. S. A.; Elkaeed, E. B.; Mehany, A. B. M.; Eissa, I. H. Discovery of new quinolines as potent colchicine binding site inhibitors: design, synthesis, docking studies, and anti-proliferative evaluation. *J. Enzyme Inhib. Med. Chem.* **2021**, *36*, 640−658.
(5) (a) Eissa, I. H.; Dahab, M. A.; Ibrahim, M. K.; Alsaif, N. A.; Alanazi, A. Z.; Eissa, S. I.; Mehany, A. B. M.; Beauchemin, A. M. Design and discovery of new antiproliferative 1,2,4-triazin-3(2H)-ones as tubulin polymerization inhibitors targeting colchicine binding site. *Bioorg. Chem.* **2021**, *112*, No. 104965. (b) El-Naggar, A. M.; Eissa, I. H.; Belal, A.; El-Sayed, A. A. Design, eco-friendly synthesis, molecular modeling and anticancer evaluation of thiazol-5(4H)-ones as potential tubulin polymerization inhibitors targeting the colchicine binding site. *RSC Adv.* **2020**, *10*, 2791−2811.
(6) Nguyen, T. L.; McGrath, C.; Hermone, A. R.; Burnett, J. C.; Zaharevitz, D. W.; Day, B. W.; Wipf, P.; Hamel, E.; Gussio, R. A Common Pharmacophore for a Diverse Set of Colchicine Site Inhibitors Using a Structure-Based Approach. *J. Med. Chem.* **2005**, *48*, 6107−6116.
(7) Ghawanmeh, A. A.; Al-Bajalan, H. M.; Mackeen, M. M.; Alali, F. Q.; Chong, K. F. Recent developments on (−)-colchicine derivatives: Synthesis and structure-activity relationship. *Eur. J. Med. Chem.* **2020**, *185*, No. 111788.
(8) (a) Singh, B.; Kumar, A.; Joshi, P.; Guru, S. K.; Kumar, S.; Wani, Z. A.; Mahajan, G.; Hussain, A.; Qazi, A. K.; Kumar, A.; Bharate, S. S.; Gupta, B. D.; Sharma, P. R.; Hamid, A.; Saxena, A. K.; Mondhe, D. M.; Bhushan, S.; Bharate, S. B.; Vishwakarma, R. A. Colchicine derivatives with potent anticancer activity and reduced P-glycoprotein induction liability. *Org. Biomol. Chem.* **2015**, *13*, 5674−5689. (b) Kim, S.-K.; Cho, S.-M.; Kim, H.; Seok, H.; Kim, S.-O.; Kyu Kwon, T.; Chang, J.-S. The colchicine derivative CT20126 shows a novel microtubule-modulating activity with apoptosis. *Exp. Mol. Med.* **2013**, *45*, No. e19. (c) Krzywik, J.; Nasulewicz-Goldeman, A.; Mozga, W.; Wietrzyk, J.; Huczyński, A. Novel Double-Modified Colchicine Derivatives Bearing 1,2,3-Triazole: Design, Synthesis, and Biological Activity Evaluation. *ACS Omega* **2021**, *6*, 26583−26600. (d) Zhang, X.; Kong, Y.; Zhang, J.; Su, M.; Zhou, Y.; Zang, Y.; Li, J.; Chen, Y.; Fang, Y.; Zhang, X.; Lu, W. Design, synthesis and biological evaluation of colchicine derivatives as novel tubulin and histone deacetylase dual inhibitors. *Eur. J. Med. Chem.* **2015**, *95*, 127−135. (e) Majcher, U.; Klejborowska, G.; Kaik, M.; Maj, E.; Wietrzyk, J.; Moshari, M.; Preto, J.; Tuszynski, J. A.; Huczyński, A. Synthesis and Biological Evaluation of Novel Triple-Modified Colchicine Derivatives as Potent Tubulin-Targeting Anticancer Agents. *Cells* **2018**, *7*, No. 216.
(9) Maroyi, A.; van der Maesen, L. J. G. *Gloriosa superba* L. (family Colchicaceae): Remedy or poison? *J. Med. Plants Res.* **2011**, *5*, 6112−6121.
(10) Jana, S.; Shekhawat, G. S. Critical review on medicinally potent plant species: *Gloriosa superba*. *Fitoterapia* **2011**, *82*, 293−301.
(11) Khan, H.; Ali Khan, M.; Mahmood, T.; Choudhary, M. I. Antimicrobial activities of *Gloriosa superba* Linn (Colchicaceae) extracts. *J. Enzyme Inhib. Med. Chem.* **2008**, *23*, 855−859.
(12) John, J.; Fernandes, J.; Nandgude, T.; Niphade, S.; Savla, A.; Deshmukh, P. Analgesic and anti-inflammatory activities of the hydroalcoholic extract from *Gloriosa superba* Linn. *Int. J. Green Pharm.* **2009**, *3*, 215−219.
(13) Bahukhandi, A.; Barola, A.; Bhatt, I. D. Impact of Solvent System on Polyphenolics and Antioxidant Activity of *Gloriosa superba* L.: Herbaceous Species of Western Himalaya. *Natl. Acad. Sci. Lett.* **2021**, *44*, 9−12.
(14) Khan, H.; Ali Khan, M.; Hussan, I. Enzyme inhibition activities of the extracts from rhizomes of *Gloriosa superba* Linn (Colchicaceae). *J. Enzyme Inhib. Med. Chem.* **2007**, *22*, 722−725.
(15) Goel, B.; Chatterjee, E.; Dey, B.; Tripathi, N.; Bhardwaj, N.; Khattri, A.; Guru, S. K.; Jain, S. K. Identification and Evaluation of Apoptosis-Inducing Activity of Ipomone from Ipomoea nil: A Novel, Unusual Bicyclo-[3.2.1] Octanone Containing Gibberic Acid Diterpenoid. *ACS Omega* **2021**, *6*, 8253−8260.
(16) Hassan, M. M. A.; Loutfy, M. A. Trioxsalen. In *Analytical Profiles of Drug Substances*; Florey, K.; Bishara, R.; Brewer, G. A.; Fairbrother, J. E.; Grady, L. T.; Leemann, H.-G.; Mollica, J. A.; Rudy, B. C., Eds.; Academic Press, 1981; Vol. *10*, pp 705−727.
(17) Morishita, H.; Iwahashi, H.; Osaka, N.; Kido, R. Chromatographic separation and identification of naturally occurring chlorogenic acids by 1H nuclear magnetic resonance spectroscopy and mass spectrometry. *J. Chromatogr. A* **1984**, *315*, 253−260.
(18) Kühnert, S. M.; Maier, M. E. Synthesis of the Core Structure of Apicularen A by Transannular Cyclization. *Org. Lett.* **2002**, *4*, 643−646.
(19) Meksuriyen, D.; Lin, L.-J.; Cordell, G. A.; Mukhopadhyay, S.; Banerjee, S. K. Nmr Studies of Colchicine and its Photoisomers, *β*- and *λ*-Lumicolchicines. *J. Nat. Prod.* **1988**, *51*, 88−93.
(20) Wang, D.; Murtaza, M.; Wood, S. A.; Mellick, G. D.; Miao, W. G.; Guymer, G. P.; Forster, P. I.; Feng, Y.; Quinn, R. J. Unbiased Phenotypic Function of Metabolites from Australia Plants Gloriosa superba and Alangium villosum against Parkinson's Disease. *Nat. Prod.* **2020**, *83*, 1440−1452.
(21) Alali, F. Q.; El-Elimat, T.; Li, C.; Qandil, A.; Alkofahi, A.; Tawaha, K.; Burgess, J. P.; Nakanishi, Y.; Kroll, D. J.; Navarro, H. A.; Falkinham, J. O.; Wani, M. C.; Oberlies, N. H. New Colchicinoids from a Native Jordanian Meadow Saffron, Colchicum brachyphyllum: Isolation of the First Naturally Occurring Dextrorotatory Colchicinoid. *J. Nat. Prod.* **2005**, *68*, 173−178.
(22) Capraro, H.-G.; Brossi, A. Tropolonic Colchicum Alkaloids. In *The Alkaloids: Chemistry and Pharmacology*; Brossi, A., Ed.; Academic Press: Orlando, Florida, 1984; Chapter 1, Vol. *23*, pp 1−70.
(23) Zarev, Y.; Foubert, K.; Ionkova, I.; Apers, S.; Pieters, L. Isolation and Structure Elucidation of Glucosylated Colchicinoids from the Seeds of *Gloriosa superba* by LC-DAD-SPE-NMR. *J. Nat. Prod.* **2017**, *80*, 1187−1191.
(24) Forbes, E. J. Colchicine and related compounds. Part XIV. Structure of *β*- and *γ*-lumicolchicine. *J. Chem. Soc.* **1955**, *0*, 3864−3870.
(25) (a) Kuncl, R. W.; Duncan, G.; Watson, D.; Alderson, K.; Rogawski, M. A.; Peper, M. Colchicine Myopathy and Neuropathy. *N. Engl. J. Med.* **1987**, *316*, 1562−1568. (b) Tochinai, R.; Suzuki, K.; Nagata, Y.; Ando, M.; Hata, C.; Komatsu, K.; Suzuki, T.; Uchida, K.; Kado, S.; Kaneko, K.; Kuwahara, M. Cardiotoxic Changes of Colchicine Intoxication in Rats: Electrocardiographic, Histopathological and Blood Chemical Analysis. *J. Toxicol. Pathol.* **2014**, *27*, 223−230.
(26) Tripathi, N.; Goel, B.; Bhardwaj, N.; Sahu, B.; Kumar, H.; Jain, S. K. Virtual screening and molecular simulation study of natural products database for lead identification of novel coronavirus main protease inhibitors. *J. Biomol. Struct. Dyn.* **2022**, *40*, 3655−3667.
(27) Sharma, R.; Guru, S. K.; Jain, S. K.; Pathania, A. S.; Vishwakarma, R. A.; Bhushan, S.; Bharate, S. B. 3-(2,6-Dichlorobenzyloxy)-11-oxo-olean-12-ene-29-oic acid, a semisynthetic derivative of glycyrrhetic acid: synthesis, antiproliferative, apoptotic and anti-angiogenesis activity. *MedChemComm* **2015**, *6*, 564−575.
(28) Morris, G. M.; Huey, R.; Lindstrom, W.; Sanner, M. F.; Belew, R. K.; Goodsell, D. S.; Olson, A. J. AutoDock4 and AutoDockTools4: Automated docking with selective receptor flexibility. *J. Comput. Chem.* **2009**, *30*, 2785−2791.
(29) Bowers, K. J.; Chow, D. E.; Xu, H.; Dror, R. O.; Eastwood, M. P.; Gregersen, B. A.; Klepeis, J. L.; Kolossvary, I.; Moraes, M. A.; Sacerdoti, F. D. In *Scalable Algorithms for Molecular Dynamics Simulations on Commodity Clusters*, SC'06: Proceedings of the 2006 ACM/IEEE Conference on Supercomputing; IEEE, 2006; p 43.
(30) John, A.; Vetrivel, D. U.; Krishnakumar, S.; Deepa, P. Comparative Modeling and Molecular Dynamics Simulation of Substrate Binding in Human Fatty Acid Synthase: Enoyl Reductase and *β*-Ketoacyl Reductase Catalytic Domains. *Genomics Inf.* **2015**, *13*, 15−24.
(31) Evans, D. J.; Holian, B. L. The Nose−Hoover thermostat. *J. Chem. Phys.* **1985**, *83*, 4069−4074.

https://doi.org/10.1021/acsomega.2c02688
ACS Omega 2022, 7, 28994−29001